30th International Conference
ENGINEERING MECHANICS 2024
Milovy, Czech Republic, May 14 – 16, 2024

INFLUENCE OF DENTAL IMPLANT INSERTION DEPTH ON STRAIN IN PERIIMPLANT BONE TISSUE

Thomková B.[*], Borák L.[**], Podešva P.[***], Podešva M.[‡], Joukal M.[‡‡], Marcián P.[‡‡‡]

Abstract: *This study investigates the influence of dental implant insertion depth on strain states within the peri-implant bone tissue. Using a finite element model based on a human mandible CT data, variations in insertion depth were simulated, ranging from 0 mm to 2 mm in 0.5 mm increments. The analysis focused on a defined volume around the implant, evaluating strain intensities categorized according to the Mechanostat hypothesis. Results revealed notable differences in strain distribution within cancellous bone with increasing insertion depth, highlighting potential implications for bone response. While cortical bone showed consistent strain patterns, variations in cancellous bone suggest a nuanced relationship between insertion depth and peri-implant bone strain.*

Keywords: Dental implant, strain states, computational modelling.

1. Introduction

The discovery of the phenomenon of osseointegration has led to significant advancements in the field of dental implantology. Modern implantology introduces new possibilities in terms of sizes, materials, and designs for dental implants. These possibilities extend beyond visual differences to also encompass techniques used for dental implant insertion. Among others, 3D imaging techniques are becoming widely employed not only for pre-insertion preparation but also during the actual implant insertion.

The effort expended during insertion is crucial not only for ensuring the problem-free function of the dental implant but also for aesthetic considerations. One widely used protocol for implant placement involves subcrestal placement, where the implant is positioned beneath the alveolar crest. The depth of insertion can vary between 0.5 mm and 3 mm below the crest (Poovarodom et al., 2023).

Mechanical strains in the bone tissue around the dental implant are influenced by the quality of the bone tissue itself, but the method and depth of insertion also play their significant roles (Chou et al., 2010; Rito-Macedo et al., 2021). From the perspective of determining strain states, the peri-implant area around the dental implant is crucial. The aim of this study is to investigate the impact of dental implant insertion depth on strain states in peri-implant bone tissue.

[*] Ing. Barbora Thomková: Institute of Solid Mechanics, Mechatronics and Biomechanics, Faculty of Mechanical Engineering, Brno University of Technology, Technická 2896/2, 616 69 Brno, Czech Republic; CZ, barbora.thomkova@vutbr.cz

[**] Ing. Libor Borák, PhD.: Institute of Solid Mechanics, Mechatronics and Biomechanics, Faculty of Mechanical Engineering, Brno University of Technology, Technická 2896/2, 616 69 Brno, Czech Republic; CZ, xmborak01@vutbr.cz

[***] Ing. Pavel Podešva: IPPON s.r.o., Dolní Jasenka 770, 755 01 Vsetín, Czech Republic; CZ, pavel.podesva@euroimplant.com

[‡] Ing. Martin Podešva: Nyrtonn s.r.o., Srbská 2741/53, Královo Pole, 612 00 Brno, Czech Republic; CZ, martin.podesva@nyrtonn.com

[‡‡] Assoc. Prof. MUDr. Marek Joukal, PhD.: Department of Anatomy, Faculty of Medicine, Masaryk University, Kamenice 126/3, 625 00 Brno, Czech Republic; CZ, mjoukal@med.muni.cz

[‡‡‡] Ing. Petr Marcián, PhD.: Institute of Solid Mechanics, Mechatronics and Biomechanics, Faculty of Mechanical Engineering, Brno University of Technology, Technická 2896/2, 616 69 Brno, Czech Republic; CZ, marcian@fme.vutbr.cz

doi: 10.21495/em2024-302

2. Methods

To assess mechanical strains in the peri-implant bone tissue resulting from dental implant loading, computational modelling using the finite element method was utilized. Specifically, Ansys software (ANSYS Academic Research Mechanical, Release 2022 R2; Swanson Analysis Systems Inc) was employed for the solution. Details regarding the development of the computational model are provided in the following subsections.

2.1. Geometry model

One human mandible was acquired from the Department of Anatomy, Faculty of Medicine, Masaryk University Brno, Czech Republic in full compliance with relevant institutional and legislative requirements. The mandible was then scanned using CT (Philips) with voxel size 0.49 mm x 0.49 mm x 0.45 mm. In total, 231 anonymized CT images were obtained. These images were processed using automatic and manual segmentation to create a model of the geometry of the typical human mandible. It should be noted that the cortical and cancellous bone tissues were segmented and modelled separately. Both bone tissue geometry models are available at 10.5281/zenodo.10636072.

The dental implant was positioned in the premolar region. Specifically, the Brånemark dental implant including the abutment (Brånemark® System Mk III Groovy (NP Ø 3.3 mm, 11.5 mm)) was utilized in all variants. The variants differed in the depth of dental implant insertion, ranging from 0 mm to 2 mm in increments by 0.5 mm (see Fig. 1). It is assumed that there is no direct contact between the abutment and the bone; hence, no abutment osseointegration was modelled. Instead, a conical gap between the abutment and the cortical bone was modelled as illustrated in Fig. 2a.

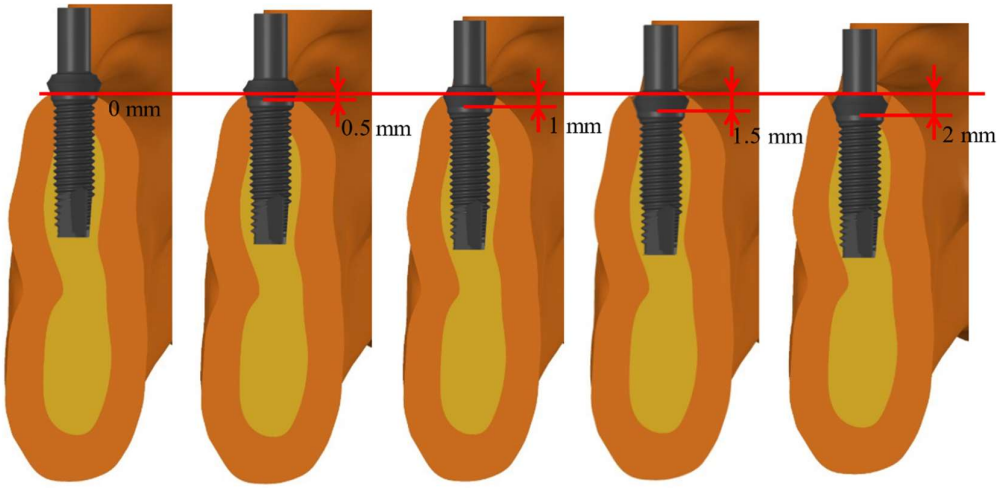

Fig. 1: Model variants with different insertion depths.

2.2. Material model

Cortical bone tissue, a portion of cancellous bone tissue and the dental implant (made of a titanium alloy) were modeled assuming a linear-elastic, homogenous, and isotropic material defined by two material characteristics, Young's modulus (E) and Poisson's ratio (μ). Specifically, E = 13 700 MPa and μ = 0.3 for cortical bone (Menicucci et al., 2002), E = 1 370 MPa and μ = 0.3 for cancellous bone, E = 110 000 MPa and μ = 0.34 for the implant (Park et al., 2022).

A portion of cancellous bone assuming a linear-elastic and isotropic material that is inhomogeneously distributed. This material model was created based on CT images data; specifically, utilizing the relationship between Hounsfield units (HU), bone density (ρ) and Young's modulus (E) (Eqs. (1) and (2)), an APDL macro was generated using the CTPixelMapper_v1-7 software application (Borák and Marcián, 2017). This macro assigns material characteristics to the nodes of the FE model (see Fig. 2b).

$$\rho = 0.114 + 0.000916 \cdot HU \; [g/cm^3] \tag{1}$$

$$E = 2349 \cdot \rho^{2.15} \; [MPa] \tag{2}$$

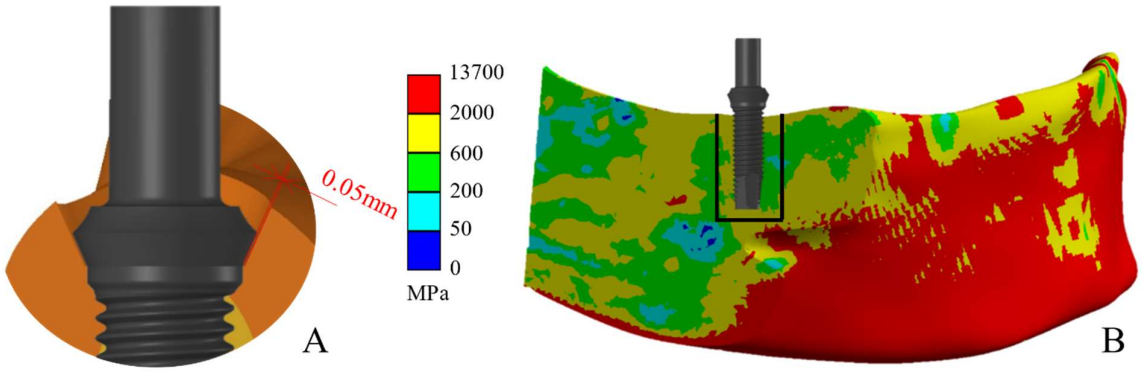

Fig. 2: a) Gap between abutment and cortical bone tissue, b) Distribution of material properties of segment of cancellous bone tissue (black lines represent VOI).

2.3. Load and boundary conditions

For the purpose of this analysis, masticatory muscle static forces were taken into account to simulate chewing. Forces and their directional vectors, as per authors Korioth and Hannam (Korioth, 1996), were incorporated into the FE model. The function of the temporomandibular joint was simulated by applying a spherical constraint to the surfaces associated with the mandibular condyles. To simulate the biting, the top of the abutment was restricted from moving in the direction of implant axis by using a remote displacement function in the FE software.

2.4. FE mesh

The geometry was meshed in Ansys using quadratic tetrahedral SOLID 187 elements, with a global element size of 0.45 mm and 0.04 mm for dental implant and areas of contact between dental implant and bone tissue, respectively. The mechanical interaction between the bone tissue and the implant was modelled using contact elements CONTA174 and TARGE170. The implant was assumed to be fully osseointegrated (i.e., a bonded contact option was used in the FE model).

3.Results and discussion

The analysis focused on strains in a limited volume of the peri-implant region of the bone. The volume of interest (VOI) was defined as a cylinder with a diameter of 6 mm around the implant and height of 18 mm from top of the abutment. Specifically, the VOIs in all variants were evaluated for strain intensity, defined as the difference between the maximum and minimum principal strains. Isolines of strain intensity for all variants can be seen in Fig. 3.

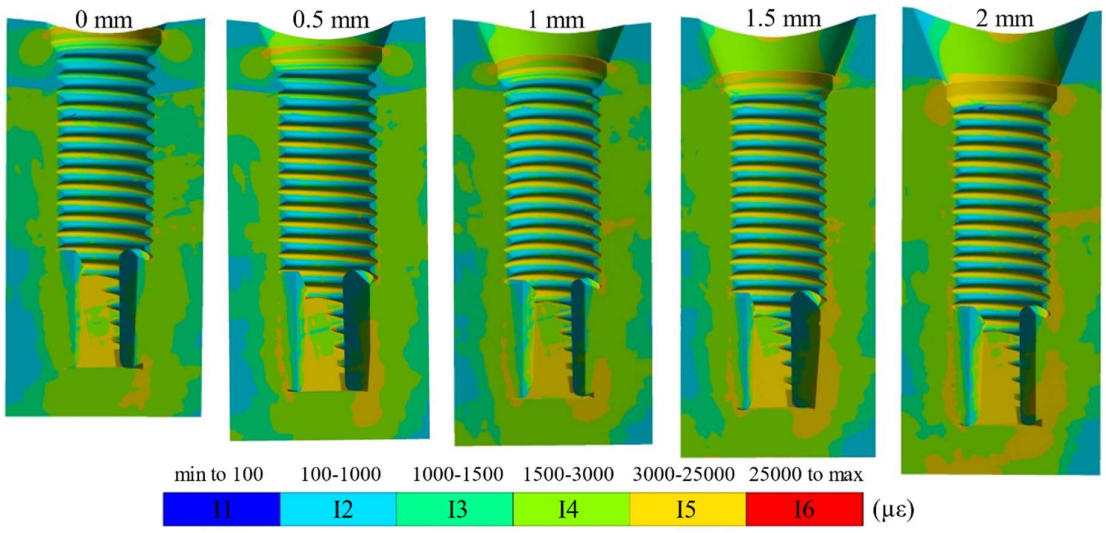

Fig. 3: Isolines of strain intensity in VOI.

Subsequently, the strain intensities in the FE nodes of the VOI were categorized using strain intervals defined by the Mechanostat hypothesis (Frost, 2004). Percentage shares of these intervals within the VOI were evaluated and compared among the variants (see Fig. 4). In particular, the intervals are defined as follows: (I1) 0–100 με, indicating no bone response; (I2) 100–1 000 με for bone resorption; (I3) 1000–1500 με and (I4) 1 500–3 000 με for bone modelling; (I5) 3 000–25 000 με for pathological overload; and the last one (I6), >25 000 με, representing the threshold for bone fracture.

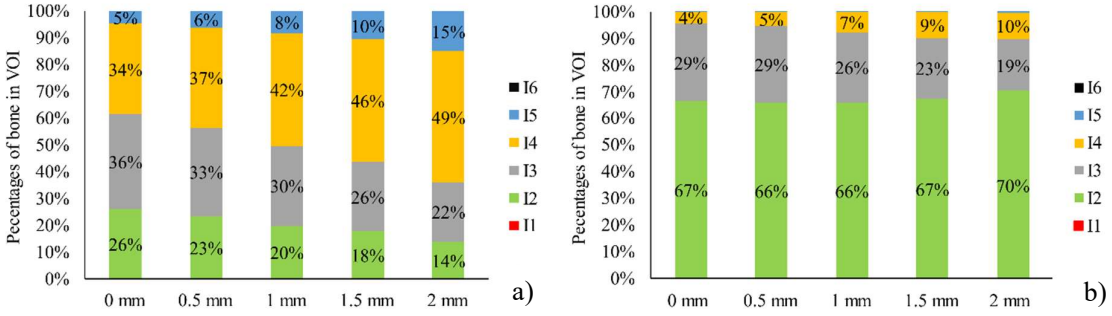

Fig. 4: Percentage of bone tissue in VOI: a) cancellous bone tissue, b) cortical bone tissue.

The difference in percentages within cortical bone tissue is not significant across all variants. Regardless of the insertion depth, the majority of strains within the VOI fall within interval I2 (67–70 %). As the insertion depth increases, the proportion of cortical bone tissue in direct contact with the dental implant decreases, leading to a slight increase of overload in the areas of contact (share of I4 in the VOI increased from 4 % to 10 %) while other tissues remain underutilized.

However, in cancellous bone, a noticeable shift in the percentages within individual intervals is observed with an increase of the insertion depth. As the depth increases, there is a noticeable increase in the shares of intervals I4 and I5, indicating a greater portion of the VOI is subjected to increased strains. Specifically, for a dental implant inserted crestally (with a 0 mm insertion depth), most of the bone tissue is distributed across intervals I3 and I4. With a 2 mm insertion depth, the predominant amount of bone tissue is found within interval I4.

Acknowledgement

This publication was supported by the project "Mechanical Engineering of Biological and Bio-inspired Systems", funded as project No. CZ.02.01.01/00/22_008/0004634 by Programme Johannes Amos Commenius, call Excellent Research. The research was supported by the specific research FSI-S-23-8240.

References

Borák, L. and Marcián, P. (2017) Inhomogeneous Material Properties Assignment to Finite Element Models of Bone: A Sensitivity Study. In: *Proc. 23rd Conference Engineering Mechanics*, Svratka, pp. 190–193.

Frost, H. M. (2004) A 2003 Update of Bone Physiology and Wolff's Law for Clinicians. *The Angle Orthodontist*, 74(1), pp. 3–15.

Chou, H., Müftü, S. and Bozkaya, D. (2010) Combined effects of implant insertion depth and alveolar bone quality on periimplant bone strain induced by a wide-diameter, short implant and a narrow-diameter, long implant. *The Journal of Prosthetic Dentistry,* 104(5), pp. 293–300.

Park, J., Park, S., Kang, I. and Noh, G. (2022) Biomechanical effects of bone quality and design features in dental implants in long-term bone stability. *Journal of Computational Design and Engineering,* 9(5), pp.1538–1548.

Korioth, T. W. P. and Hannam, A. G. (1996) Deformation of the Human Mandible During Simulated Tooth Clenching. *Journal of Dental Research,* 73(1), pp. 56–66.

Menicucci, G., Mossolov, A., Mozzati, M., Lorenzetti, M. and Preti, G. (2002) Tooth-implant connection: some biomechanical aspects based on finite element analyses. *Clinical Oral Implants Research,* 13(3), pp. 334–341.

Poovarodom, P. et al. (2023) Effect of implant placement depth on bone remodeling on implant-supported single zirconia abutment crown: A 3D finite element study. *Journal of Prosthodontic Research*, 67(2), pp. 278–287.

Rito-Macedoet, F. et al. (2021) Implant insertion angle and depth: Peri-implant bone stress analysis by the finite element method. *Journal of Clinical and Experimental Dentistry*, 13(12), pp. 1167–1173.